

Proceedings of International Conference on Technology and Social Science 2020

(ICTSS 2020)

Dec. 3, 2020

Phase Margin Test for Power-Stage of DC-DC Buck Converter

MinhTri Tran*, Yasunori Kobori, Anna Kuwana,
and Haruo Kobayashi

Gunma University, Japan



Outline

1. Research Background

- Motivation, objectives and achievements
- Characteristics of an adaptive feedback network

2. Analysis of Power-Stage of DC-DC Converter

- Operating regions of 2nd-order systems
- Phase margin of power-stage of DC-DC converter

3. Ripple Reduction for DC-DC Converters

- LC Harmonic Notch filter
- Nichols chart of power stage of buck converter

4. Conclusions

1. Research Background

Noise in Electronic Systems

Performance of a system

Signal to
Noise Ratio:

$$\text{SNR} = \frac{\text{Signal power}}{\text{Noise power}}$$

Common types of noise:

- Electronic noise
- Thermal noise,
- Intermodulation noise,
- Cross-talk,
- Impulse noise,
- Shot noise, and
- Transit-time noise.



Performance of a device

Figure of
Merit:

$$F = \frac{\text{Output SNR}}{\text{Input SNR}}$$

Device noise:

- Flicker noise,
- Thermal noise,
- White noise.

DC-DC converters

- **Overshoot,**
- **Ringing**
- **Ripple**

1. Research Background

Effects of Ripple and Ringing on Electronic Systems

- **Ringing** is **overshoot/undershoot voltage** or current when it's seen on time domain.
- **Ripple** is **wasted power**, and **has many undesirable effects on analog circuits**.

Ringing does the following things:

- **Causes** EMI noise,
- **Heats** components,
- **Consumes** the power,
- **Decreases the** performance,
- **Damages** the devices.

Ripple does the following things:

- **Increases** current flow,
- **Increases** noise,
- **Creates** the distortion,
- **Causes** digital circuits to operate improperly.

1. Research Background

Objectives of Study

- **Investigation of behaviors of power-stage of DC-DC converters**
- **Ripple reduction for DC-DC buck converter using LC Harmonic Notch filter**
- **Measurement of self-loop function in power-stage of DC-DC buck converter**
- **Observation of phase margin at unity gain on the Nichols chart**

1. Research Background

Achievements of Study

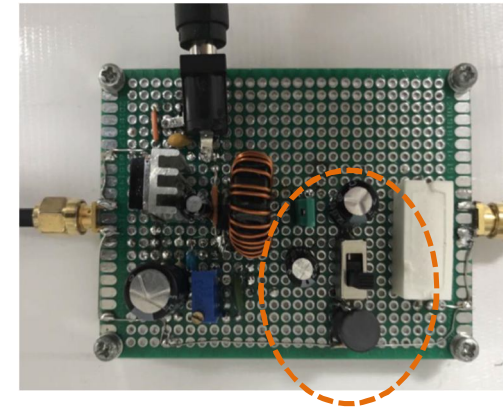
Alternating current conservation
for deriving self-loop function

$$L(\omega) = -\frac{V_{inc}}{V_{trans}}$$



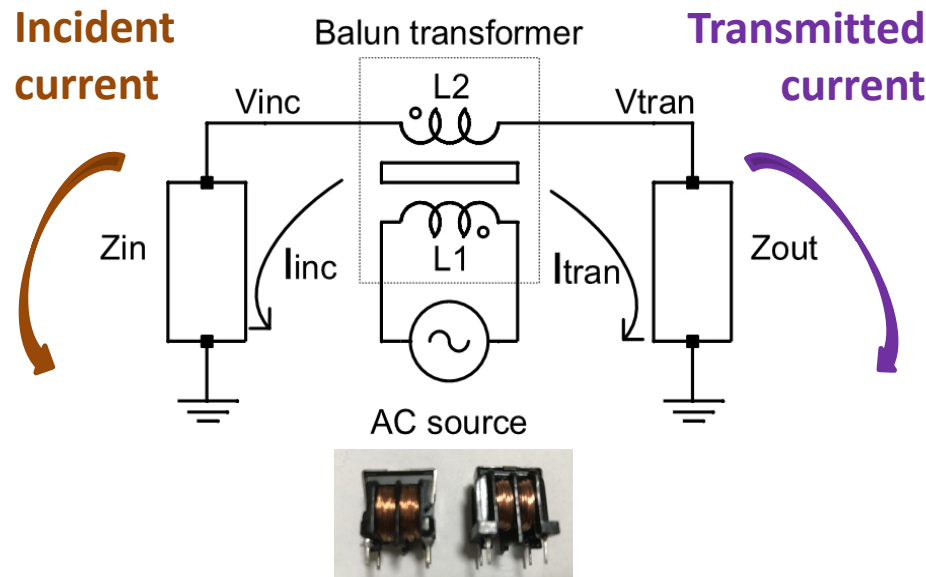
Stability test for
power-stage

Implemented circuit

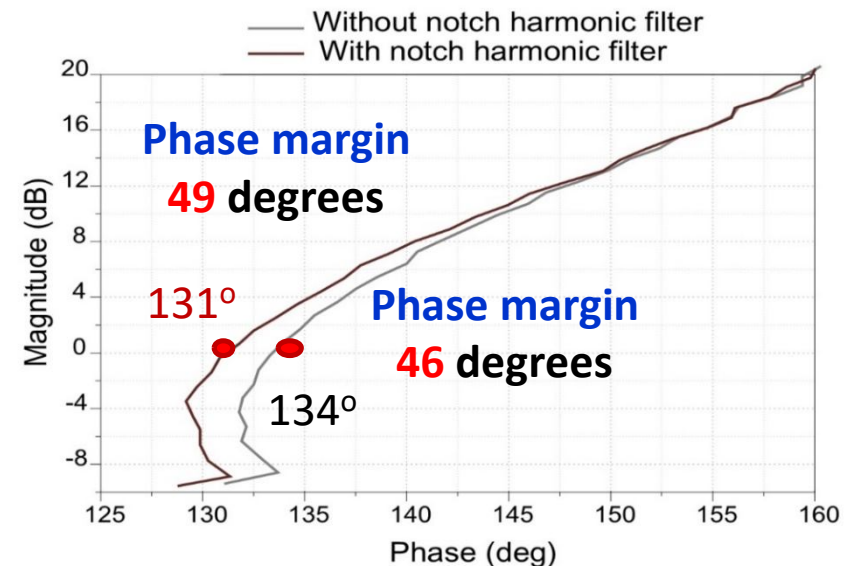


LC
notch
filter

Derivation of self-loop function



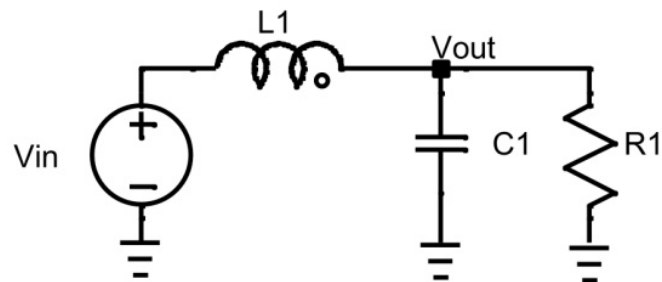
Phase margin of power stage



1. Research Background

Approaching Methods

Simplified power-stage

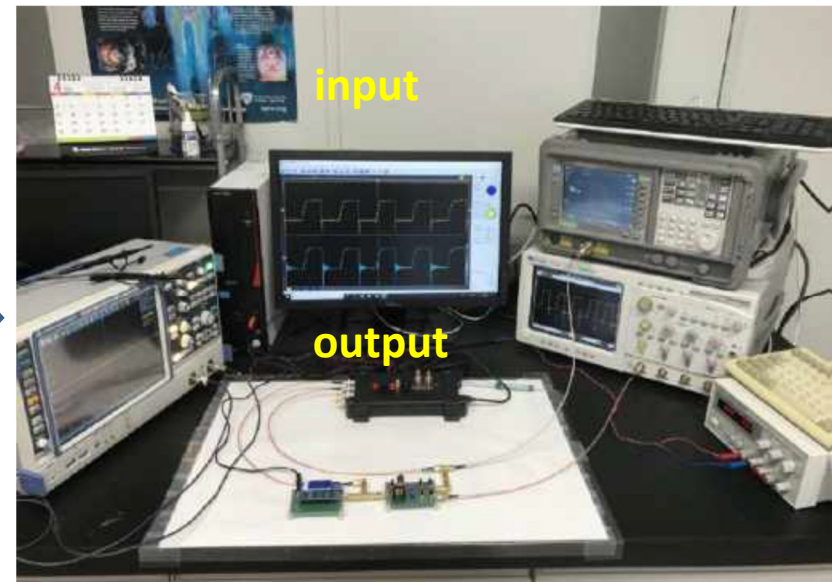
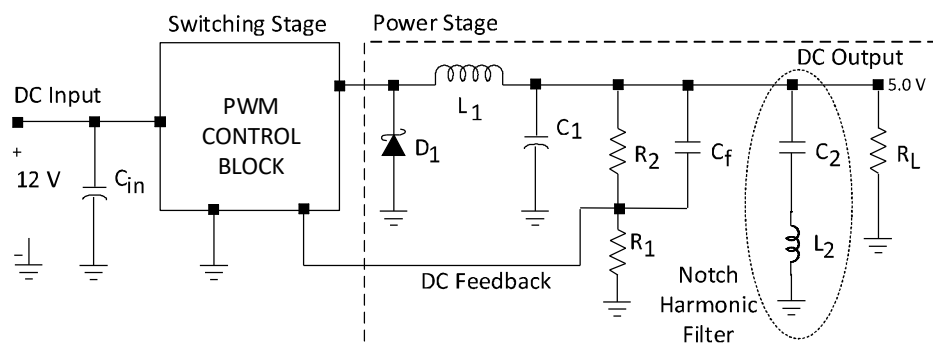


Balun transformer



Measurement set up

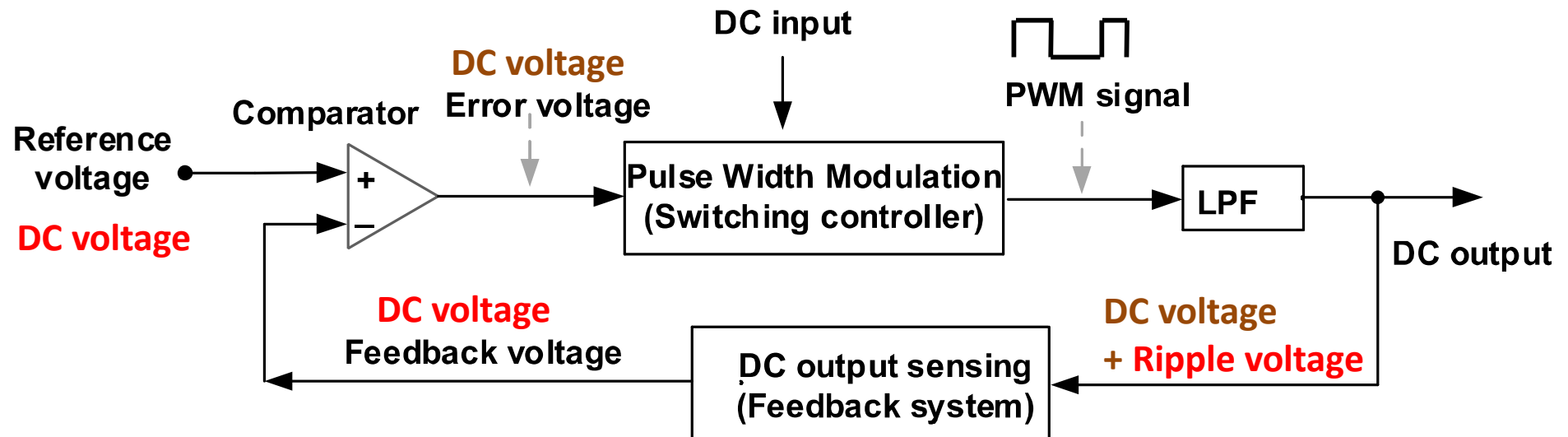
Design of DC-DC buck converter



1. Research Background

Characteristics of Adaptive Feedback Network

Block diagram of a typical adaptive feedback system



Adaptive feedback is used to control the output source along with the decision source (**DC-DC Buck converter**).

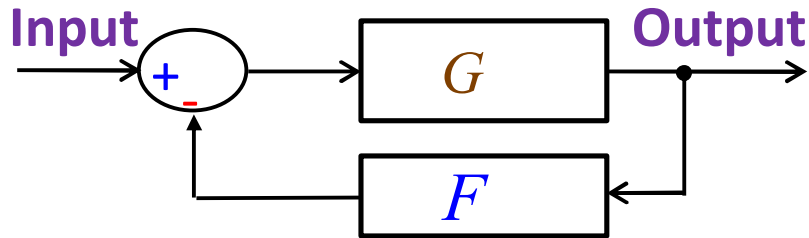
Transfer function of an **adaptive feedback network** is **significantly different from** transfer function of a **linear negative feedback network**.

→ **Loop gain is independent** of frequency variable (**referent voltage, feedback voltage, and error voltage are DC voltages**).

1. Research Background

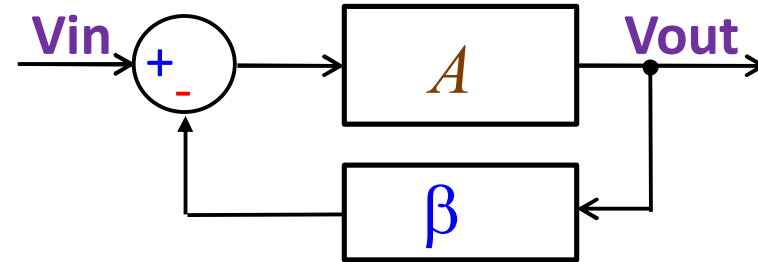
Loop Gain in Feedback Control Systems

Adaptive feedback systems



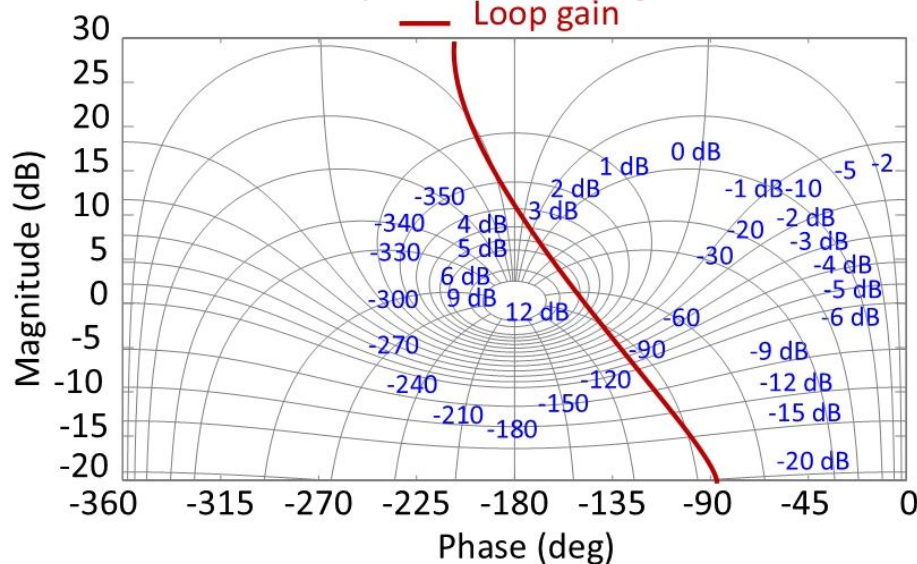
Transfer function $H = \frac{G}{1 + GF} \approx 1$
GF : loop gain

Inverting amplifier

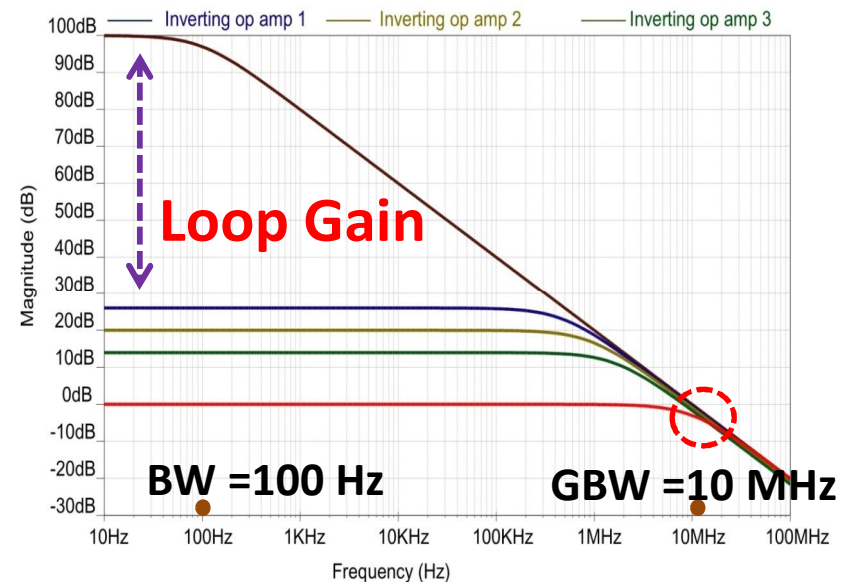


Transfer function $H = \frac{A}{1 + A\beta} \approx \frac{1}{\beta}$
Aβ : loop gain

Nichols plot of loop gain



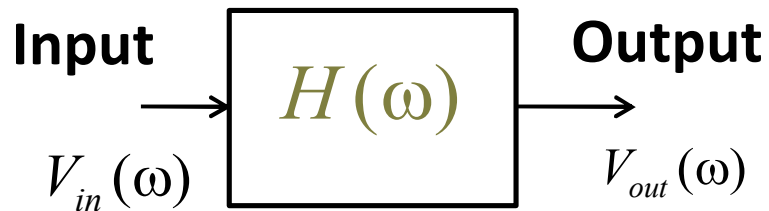
Gain reduction



1. Research Background

Self-loop Function in A Transfer Function

Linear system



Model of a linear system

$$H(\omega) = \frac{b_0(j\omega)^n + \dots + b_{n-1}(j\omega) + b_n}{a_0(j\omega)^n + \dots + a_{n-1}(j\omega) + a_n}$$

Transfer function

$$H(\omega) = \frac{V_{out}(\omega)}{V_{in}(\omega)} = \frac{A(\omega)}{1 + L(\omega)}$$

$A(\omega)$: Numerator function

$H(\omega)$: Transfer function

$L(\omega)$: Self-loop function

Variable: angular frequency (ω)

○ Polar chart → Nyquist chart

○ Magnitude-frequency plot

○ Angular-frequency plot

○ Magnitude-angular diagram → Nichols diagram

Bode plots

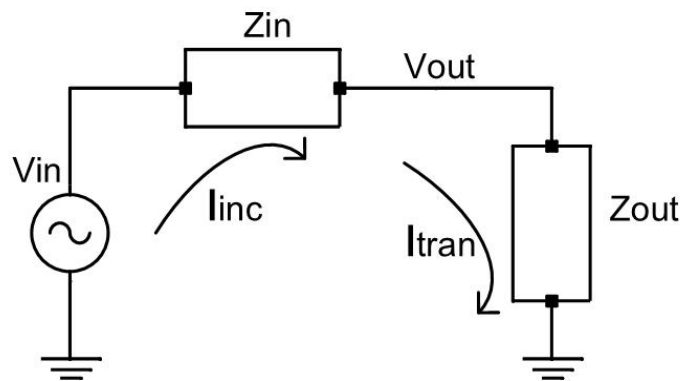
1. Research Background

Alternating Current Conservation

Transfer function

$$H(\omega) = \frac{V_{out}(\omega)}{V_{in}(\omega)} = \frac{1}{1 + \frac{Z_{in}}{Z_{out}}}$$

$$\Rightarrow L(\omega) = \frac{Z_{in}}{Z_{out}};$$



Simplified linear system

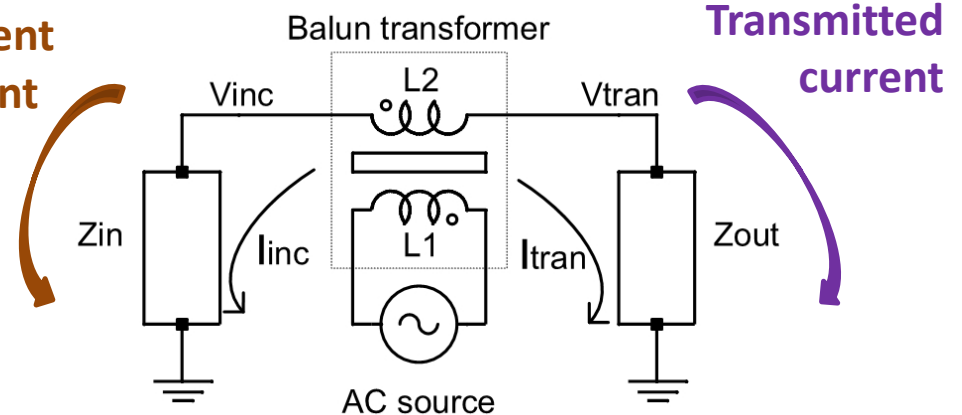
Self-loop function

$$\frac{V_{inc}}{Z_{in}} = -\frac{V_{trans}}{Z_{out}} \Rightarrow L(\omega) = -\frac{V_{inc}}{V_{trans}} = \frac{Z_{in}}{Z_{out}}$$



10 mH
inductance

Incident
current



Derivation of self-loop function

1. Research Background

Limitations of Conventional Methods

- **Middlebrook's measurement of loop gain**
 - Applying only in feedback systems (**DC-DC converters**).
- **Replica measurement of loop gain**
 - Using two identical networks (**not real measurement**).
- **Nyquist's stability condition**
 - Theoretical analysis for feedback systems (**Lab tool**).
- **Nichols chart of loop gain**
 - Only used in feedback control theory (**Lab tool**).

Outline

1. Research Background

- Motivation, objectives and achievements
- Characteristics of an adaptive feedback network

2. Analysis of Power-Stage of DC-DC Converter

- Operating regions of 2nd-order systems
- Phase margin of power-stage of DC-DC converter

3. Ripple Reduction for DC-DC Converters

- LC Harmonic Notch filter
- Nichols chart of power stage of buck converter

4. Conclusions

2. Analysis of Power-Stage of DC-DC Converter Behaviors of Second-order Transfer Function

Second-order transfer function:
$$H(\omega) = \frac{1}{1 + a_0(j\omega)^2 + a_1j\omega}$$

Case	Over-damping	Critically damping	Under-damping
Delta (Δ)	$\frac{1}{a_0} < \left(\frac{a_1}{2a_0}\right)^2 \Rightarrow \Delta = a_1^2 - 4a_0 > 0$	$\frac{1}{a_0} = \left(\frac{a_1}{2a_0}\right)^2 \Rightarrow \Delta = a_1^2 - 4a_0 = 0$	$\frac{1}{a_0} > \left(\frac{a_1}{2a_0}\right)^2 \Rightarrow \Delta = a_1^2 - 4a_0 < 0$
Module $ H(\omega) $	$\frac{1}{a_0} \sqrt{\omega^2 + \left(\frac{a_1}{2a_0} - \sqrt{\left(\frac{a_1}{2a_0}\right)^2 - \frac{1}{a_0}}\right)^2} \sqrt{\omega^2 + \left(\frac{a_1}{2a_0} + \sqrt{\left(\frac{a_1}{2a_0}\right)^2 - \frac{1}{a_0}}\right)^2}$	$\frac{1}{a_0} \sqrt{\omega^2 + \left(\frac{a_1}{2a_0}\right)^2} = \frac{1}{2} = -6dB$	$\frac{1}{a_0} \sqrt{\left(\omega - \sqrt{\frac{1}{a_0} - \left(\frac{a_1}{2a_0}\right)^2}\right)^2 + \left(\frac{a_1}{2a_0}\right)^2} \sqrt{\left(\omega + \sqrt{\frac{1}{a_0} - \left(\frac{a_1}{2a_0}\right)^2}\right)^2 + \left(\frac{a_1}{2a_0}\right)^2}$
Angular $\theta(\omega)$	$-\arctan\left(\frac{\omega}{\frac{a_1}{2a_0} - \sqrt{\left(\frac{a_1}{2a_0}\right)^2 - \frac{1}{a_0}}}\right) - \arctan\left(\frac{\omega}{\frac{a_1}{2a_0} + \sqrt{\left(\frac{a_1}{2a_0}\right)^2 - \frac{1}{a_0}}}\right)$	$-2 \arctan\left(\frac{2a_0\omega}{a_1}\right)$	$-\arctan\left(\frac{\omega - \sqrt{\frac{1}{a_0} - \left(\frac{a_1}{2a_0}\right)^2}}{\frac{a_1}{2a_0}}\right) - \arctan\left(\frac{\omega + \sqrt{\frac{1}{a_0} - \left(\frac{a_1}{2a_0}\right)^2}}{\frac{a_1}{2a_0}}\right)$
$\omega_{cut} = \frac{a_1}{2a_0}$	$ H(\omega_{cut}) < \frac{2a_0}{a_1}$ $\theta(\omega_{cut}) > -\frac{\pi}{2}$	$ H(\omega_{cut}) = \frac{2a_0}{a_1}$ $\theta(\omega_{cut}) = -\frac{\pi}{2}$	$ H(\omega_{cut}) > \frac{2a_0}{a_1}$ $\theta(\omega_{cut}) < -\frac{\pi}{2}$

2. Analysis of Power-Stage of DC-DC Converter Behaviors of Second-order Self-loop Function

Second-order self-loop function: $L(\omega) = j\omega[a_0 j\omega + a_1]$

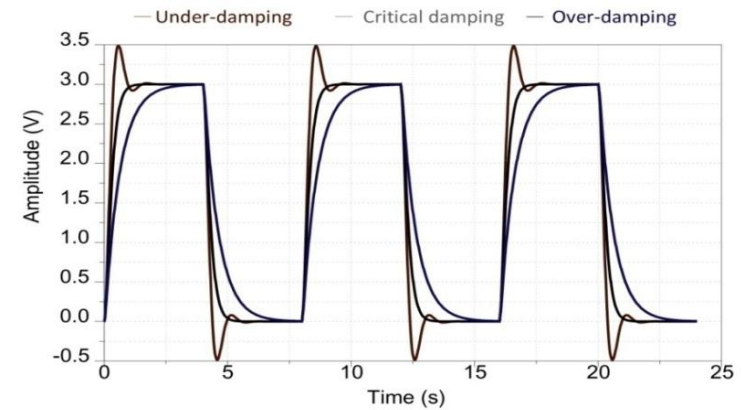
Case	Over-damping	Critical damping	Under-damping
Delta (Δ)	$\Delta = a_1^2 - 4a_0 > 0$	$\Delta = a_1^2 - 4a_0 = 0$	$\Delta = a_1^2 - 4a_0 < 0$
$ L(\omega) $	$\omega\sqrt{(a_0\omega)^2 + a_1^2}$	$\omega\sqrt{(a_0\omega)^2 + a_1^2}$	$\omega\sqrt{(a_0\omega)^2 + a_1^2}$
$\theta(\omega)$	$\frac{\pi}{2} + \arctan \frac{a_0\omega}{a_1}$	$\frac{\pi}{2} + \arctan \frac{a_0\omega}{a_1}$	$\frac{\pi}{2} + \arctan \frac{a_0\omega}{a_1}$
$\omega_1 = \frac{a_1}{2a_0}\sqrt{\sqrt{5}-2}$	$ L(\omega_1) > 1$ $\pi - \theta(\omega_1) > 76.3^\circ$	$ L(\omega_1) = 1$ $\pi - \theta(\omega_1) = 76.3^\circ$	$ L(\omega_1) < 1$ $\pi - \theta(\omega_1) < 76.3^\circ$
$\omega_2 = \frac{a_1}{2a_0}$	$ L(\omega_2) > \sqrt{5}$ $\pi - \theta(\omega_2) > 63.4^\circ$	$ L(\omega_2) = \sqrt{5}$ $\pi - \theta(\omega_2) = 63.4^\circ$	$ L(\omega_2) < \sqrt{5}$ $\pi - \theta(\omega_2) < 63.4^\circ$
$\omega_3 = \frac{a_1}{a_0}$	$ L(\omega_3) > 4\sqrt{2}$ $\pi - \theta(\omega_3) > 45^\circ$	$ L(\omega_3) = 4\sqrt{2}$ $\pi - \theta(\omega_3) = 45^\circ$	$ L(\omega_3) < 4\sqrt{2}$ $\pi - \theta(\omega_3) < 45^\circ$

2. Analysis of Power-Stage of DC-DC Converter

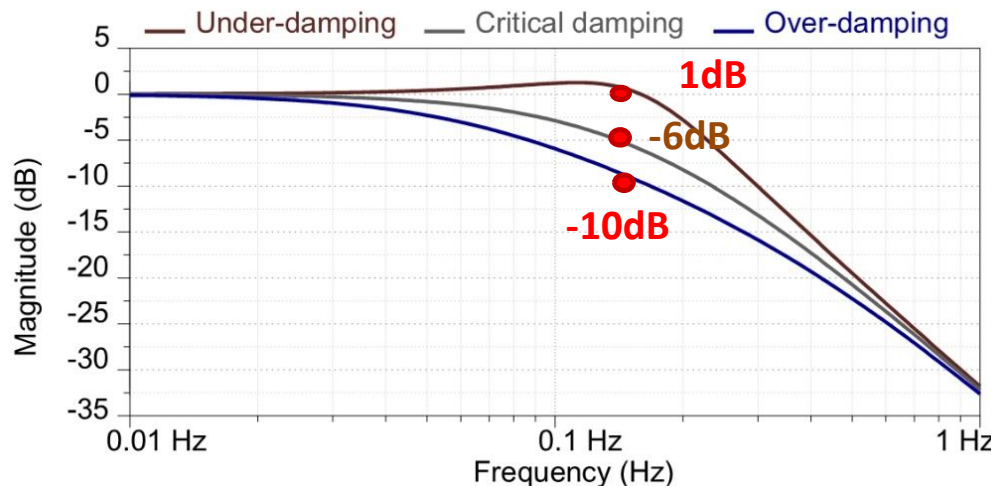
Operating Regions of 2nd-Order System

- Under-damping:** $H_1(\omega) = \frac{1}{(j\omega)^2 + j\omega + 1}$;
 $L_1(\omega) = (j\omega)^2 + j\omega$;
- Critical damping:** $H_2(\omega) = \frac{1}{(j\omega)^2 + 2j\omega + 1}$;
 $L_2(\omega) = (j\omega)^2 + 2j\omega$;
- Over-damping:** $H_3(\omega) = \frac{1}{(j\omega)^2 + 3j\omega + 1}$;
 $L_3(\omega) = (j\omega)^2 + 3j\omega$;

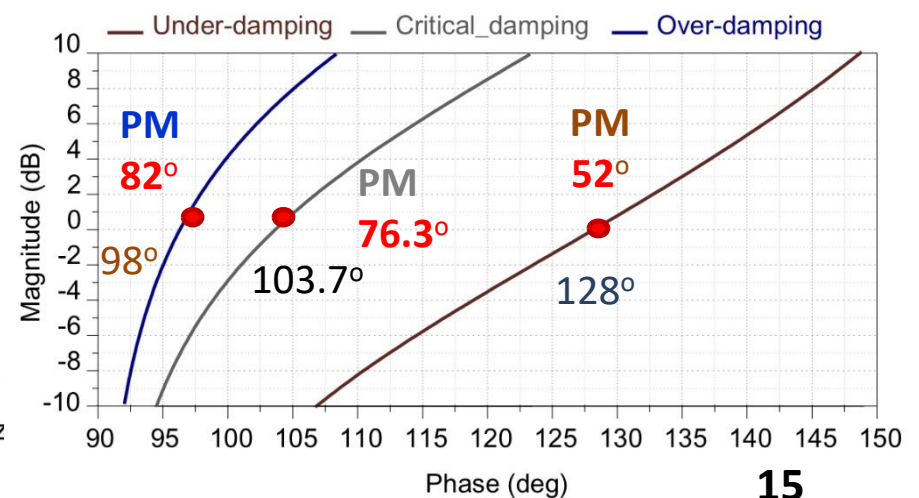
Transient response



Bode plot of transfer function

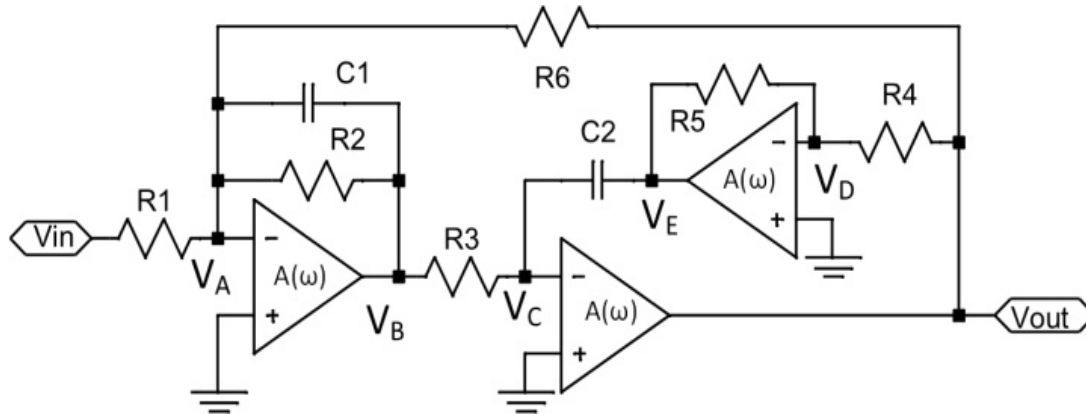


Nichols plot of self-loop function



2. Analysis of Power-Stage of DC-DC Converter Implemented Circuit of Åkerberg-Mossberg LPF

Schematic of Åkerberg-Mossberg LPF



Transfer function & self-loop function

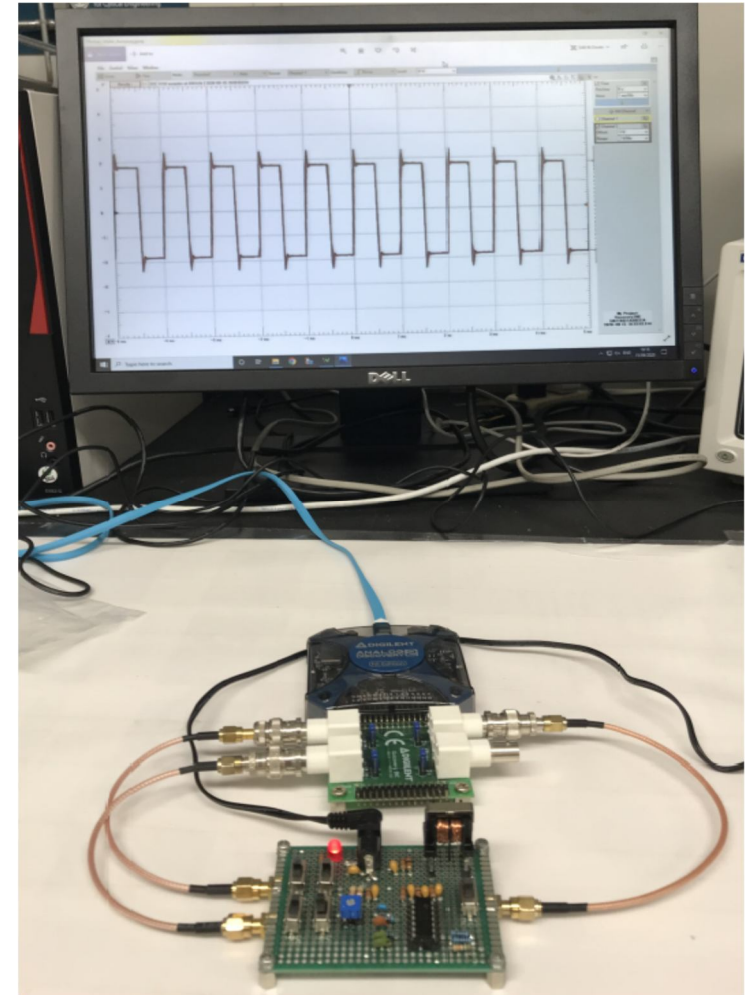
$$H(\omega) = -\frac{b_0}{a_0(j\omega)^2 + a_1j\omega + 1};$$

$$L(\omega) = a_0(j\omega)^2 + a_1j\omega;$$

where, $b_0 = \frac{R_6}{R_1};$

$$a_0 = \frac{R_3}{R_4} R_5 R_6 C_1 C_2; a_1 = \frac{R_3 R_5 R_6}{R_4 R_2} C_2;$$

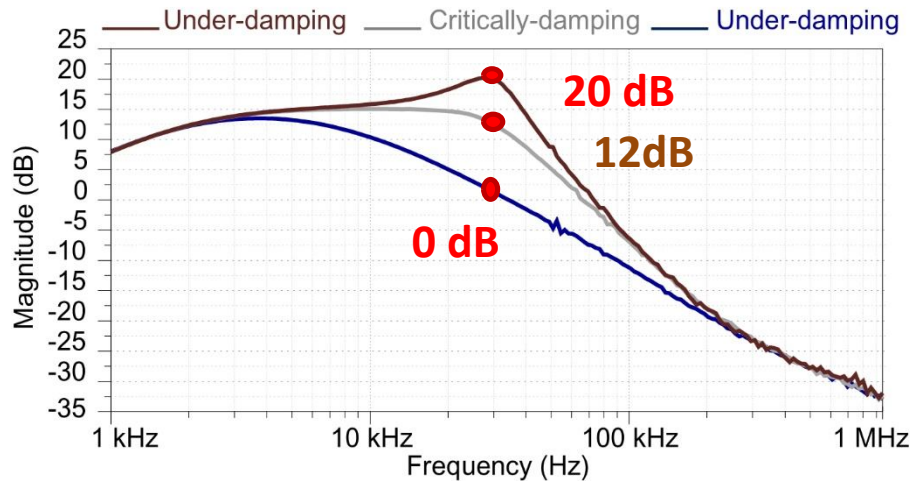
Measurement set up



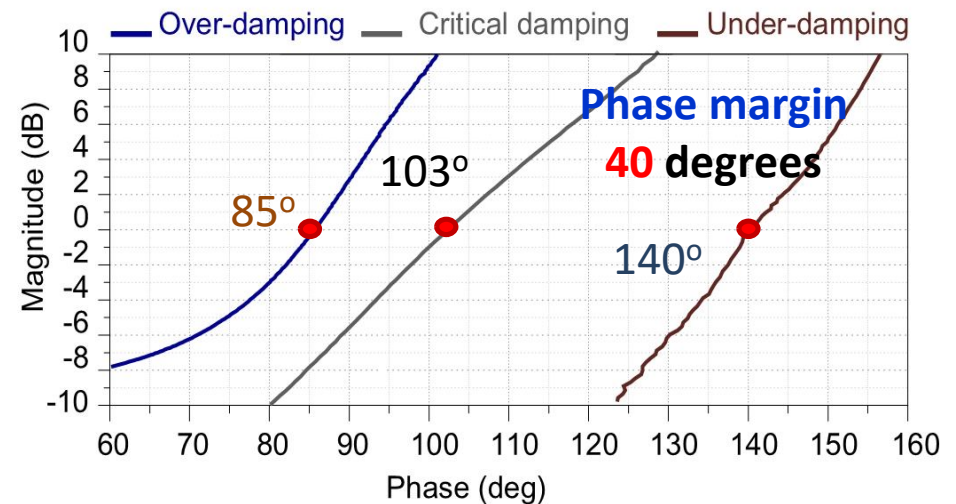
2. Analysis of Power-Stage of DC-DC Converter

Measurement Results of Åkerberg-Mossberg LPF

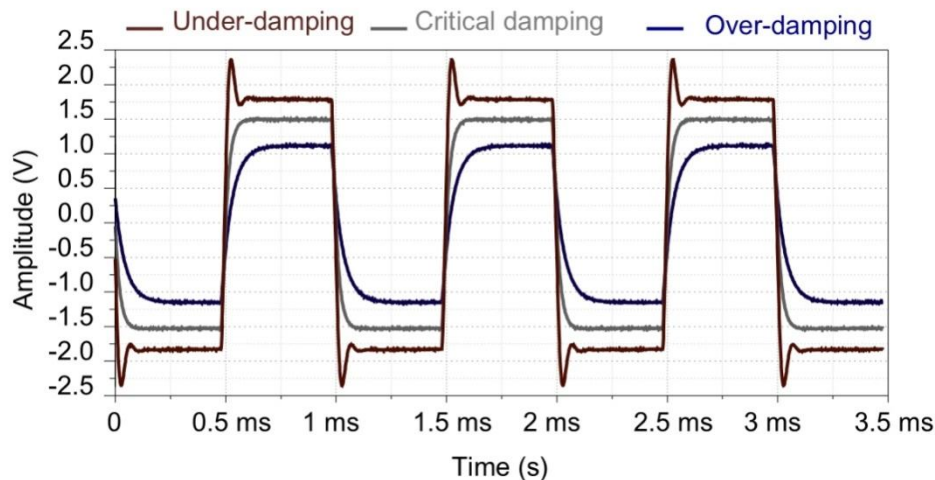
Bode plot of transfer function



Nichols plot of self-loop function



Transient response



Over-damping:

→ Phase margin is **95** degrees.

Critical damping:

→ Phase margin is **77** degrees.

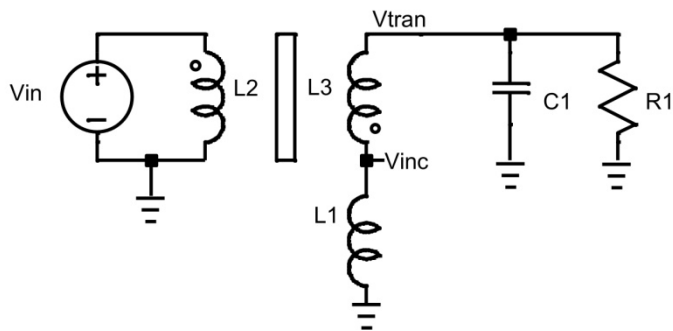
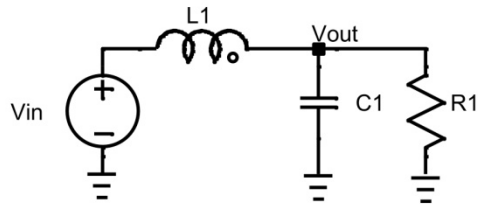
Under-damping:

→ Phase margin is **40** degrees.

2. Analysis of Power-Stage of DC-DC Converter

Behaviors of power-stage of DC-DC Converter

Parallel RLC low-pass filter



Transfer function & self-loop function:

$$H(\omega) = \frac{V_{out}}{V_{in}} = \frac{1}{1 + a_0 (j\omega)^2 + a_1 j\omega};$$

$$L(\omega) = a_0 (j\omega)^2 + a_1 j\omega;$$

Where: $a_0 = LC$; $a_1 = \frac{L}{R}$;

$$\omega_0 = 1/\sqrt{LC};$$

$$|Z_L| = \omega_0 L; \quad |Z_C| = 1/\omega_0 C;$$

Operating regions

• **Over-damping:** $\frac{1}{LC} < \left(\frac{R}{2L}\right)^2 \Leftrightarrow |Z_L| = |Z_C| < R/2$

• **Critical damping:** $\frac{1}{LC} = \left(\frac{R}{2L}\right)^2 \Leftrightarrow |Z_L| = |Z_C| = R/2$

• **Under-damping:** $\frac{1}{LC} > \left(\frac{R}{2L}\right)^2 \Leftrightarrow |Z_L| = |Z_C| > R/2$

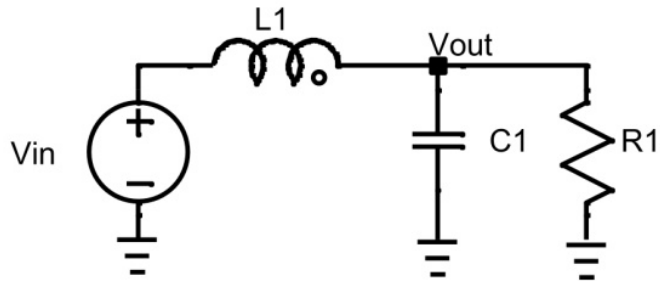
$$|Z_L| = |Z_C| = 2R$$

Balanced charging-
discharging time condition

2. Analysis of Power-Stage of DC-DC Converter

Phase Margin of Power-Stage of DC-DC Converter

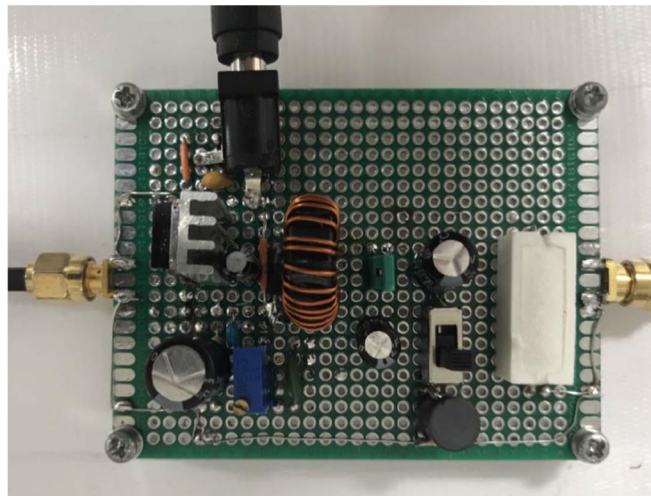
Simplified power-stage



$L_1 = 220 \mu\text{H}$, $C_1 = 100 \mu\text{F}$, $R_1 = 5 \Omega$,

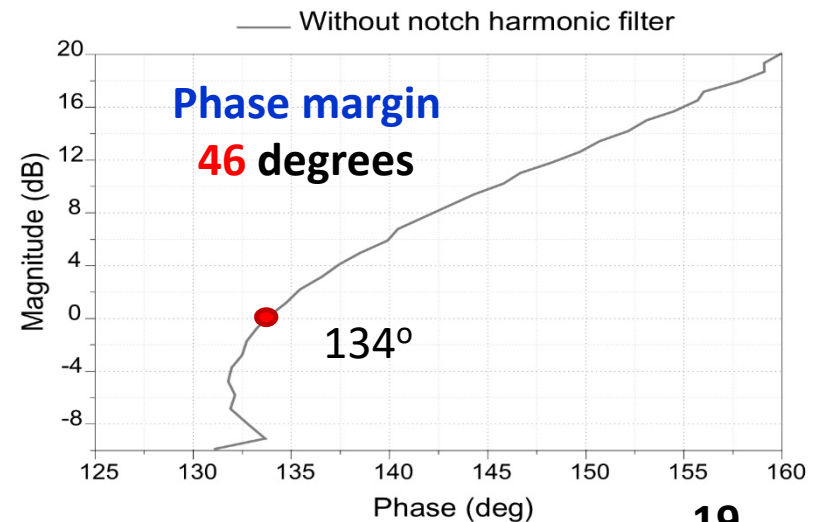
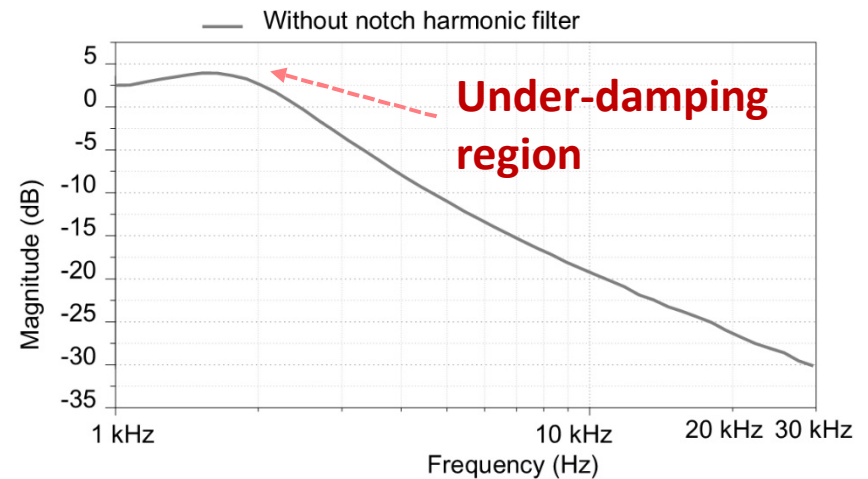
Bode plot of transfer function

Implemented circuit



Nichols plot of self-loop function

Measured results



Outline

1. Research Background

- Motivation, objectives and achievements
- Characteristics of an adaptive feedback network

2. Analysis of Power-Stage of DC-DC Converter

- Operating regions of 2nd-order systems
- Phase margin of power-stage of DC-DC converter

3. Ripple Reduction for DC-DC Converters

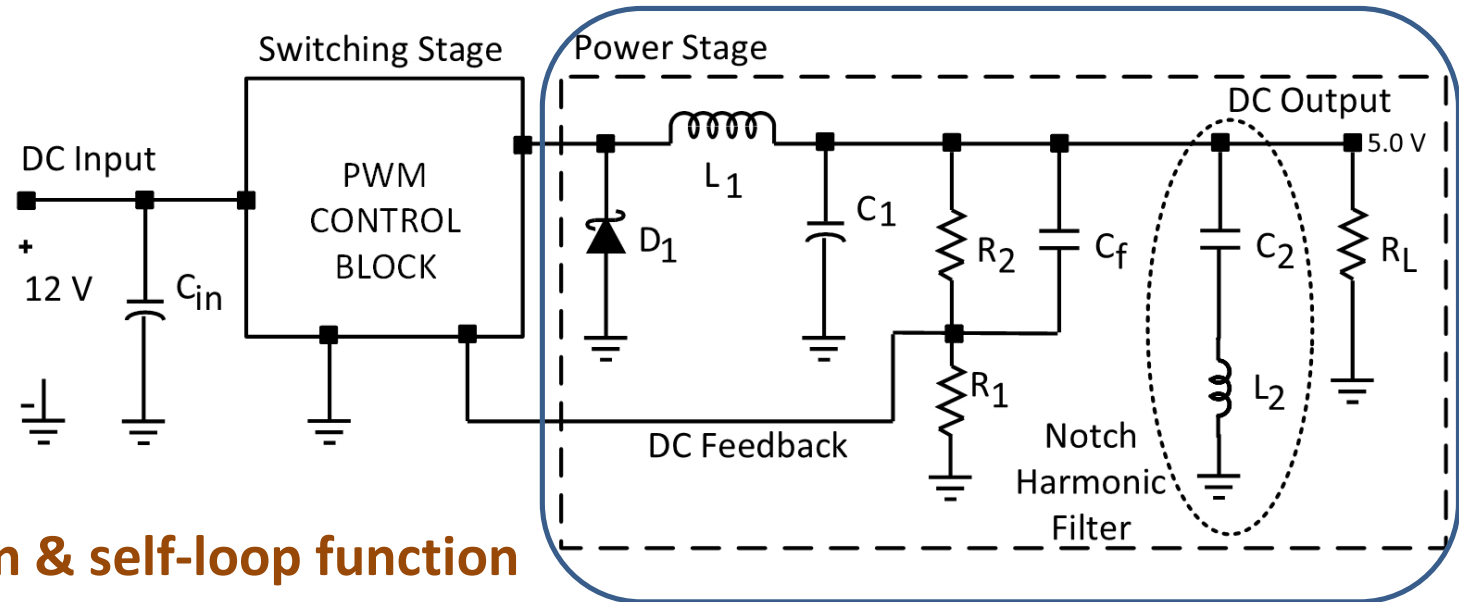
- LC Harmonic Notch filter
- Nichols chart of power stage of buck converter

4. Conclusions

3. Ripple Reduction for DC-DC Converters

Ripple Reduction using LC Harmonic Notch Filter

Schematic diagram of DC-DC buck converter



Transfer function & self-loop function

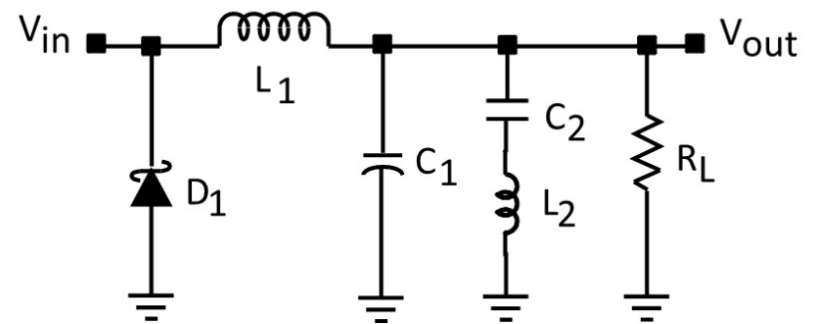
$$H(\omega) = \frac{b_0(j\omega)^2 + 1}{a_0(j\omega)^4 + a_1(j\omega)^3 + a_2(j\omega)^2 + a_3j\omega + 1}$$

$$L(\omega) = a_0(j\omega)^4 + a_1(j\omega)^3 + a_2(j\omega)^2 + a_3j\omega$$

Where, $b_0 = L_2C_2; a_0 = L_1C_1L_2C_2;$

$$a_1 = \frac{L_1L_2C_2}{R_L}; a_2 = L_1C_1 + L_2C_2 + L_1C_2; a_3 = \frac{L_1}{R_L};$$

Simplified model of power-stage



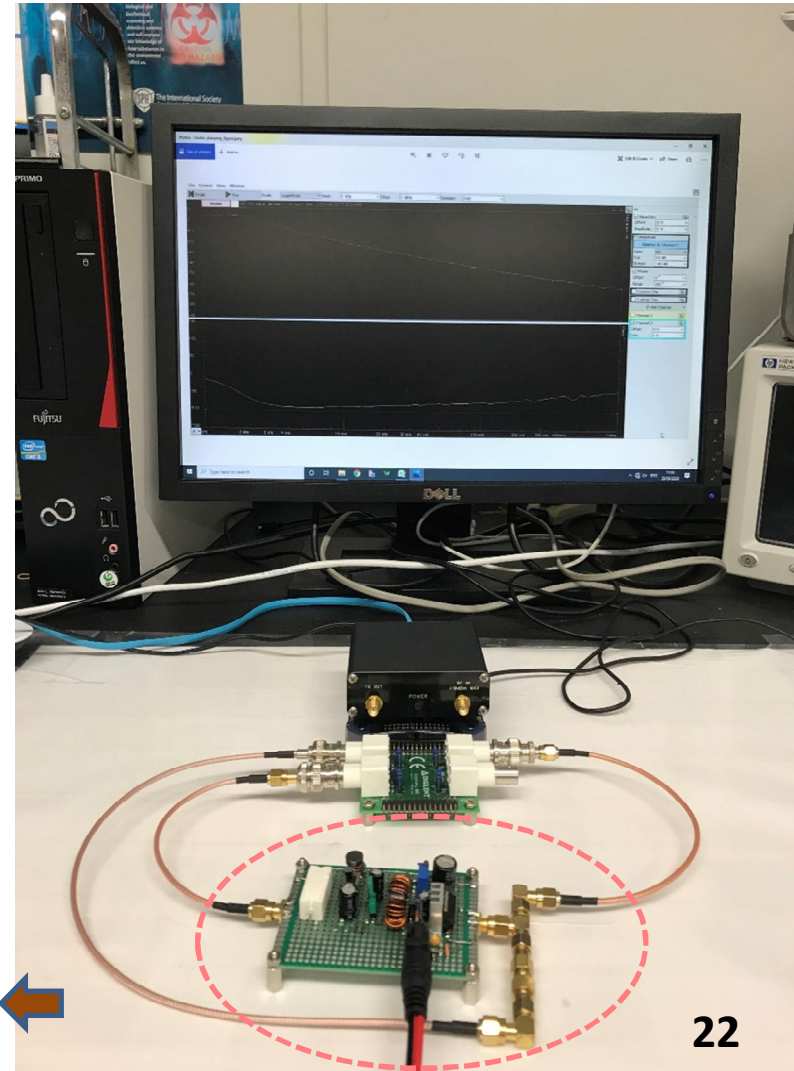
3. Ripple Reduction for DC-DC Converters

Implemented Circuit for DC-DC Converter

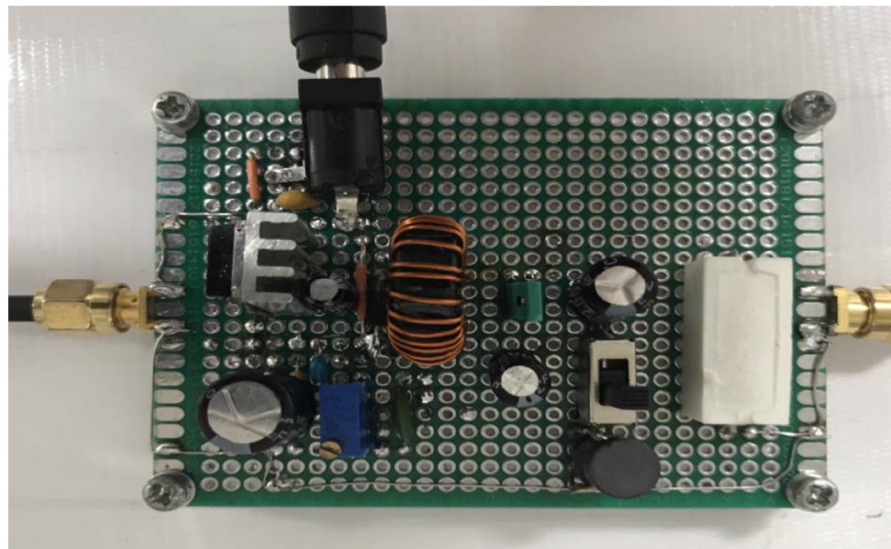
Design parameters

Input voltage (V_{in})	12 V
Output voltage (V_o)	5.0 V
Output current (I_o)	1 A
Clock frequency (F_{ck})	180 kHz
Output ripple	< 10 mVpp

Measurement set up



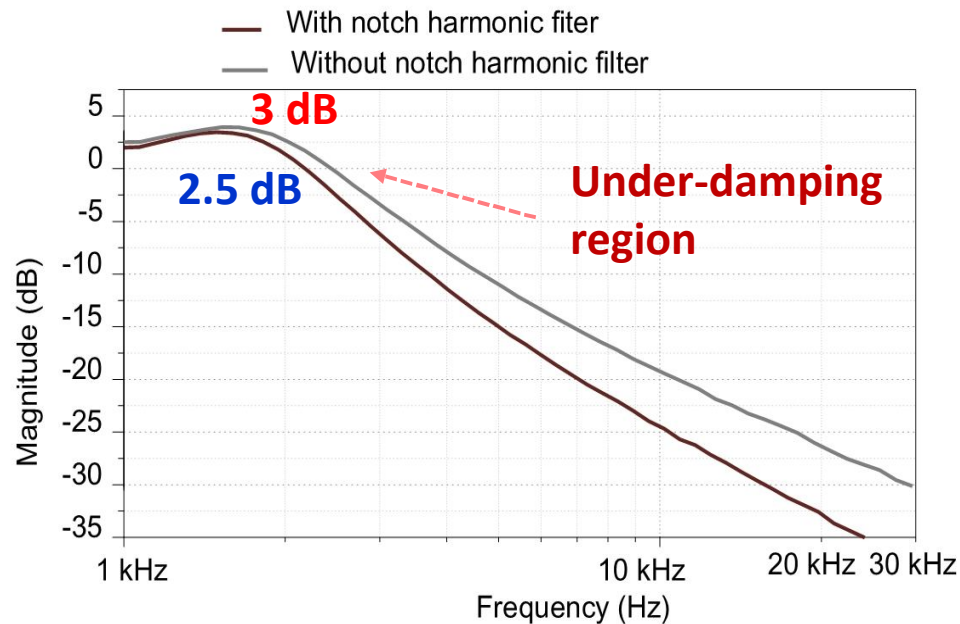
Implemented circuit



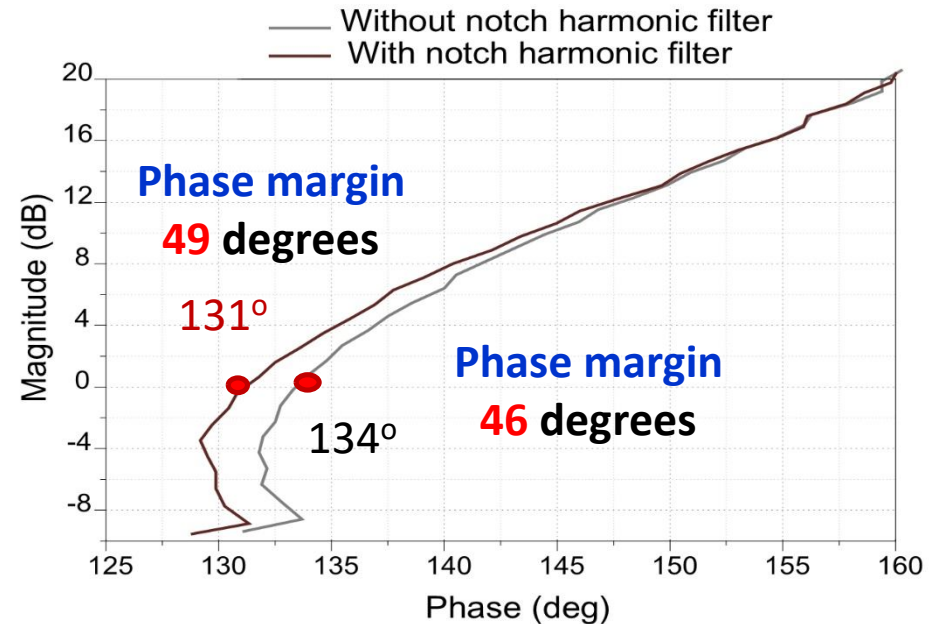
3. Ripple Reduction for DC-DC Converters

Measurement Results of Proposed Design Circuit

Bode plot of transfer function



Nichols plot of self-loop function



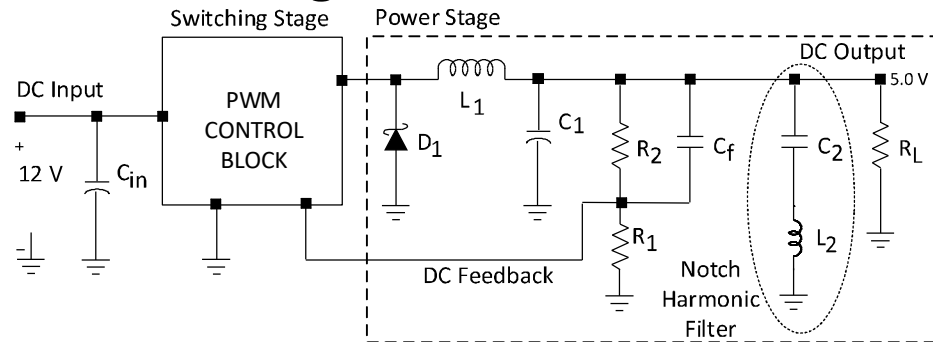
- Reduce the cut-off frequency of the power-stage
- Reduce the ripple caused by high-order harmonic signals

- Improvement of phase margin of the power-stage
- Reduce the overshoot caused by the passive components

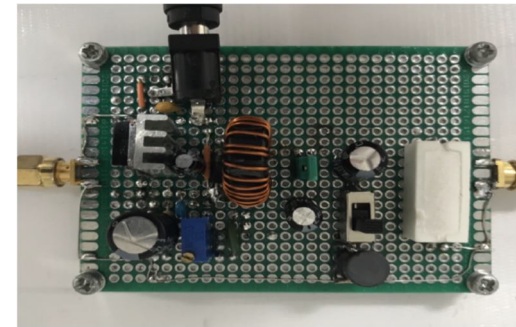
3. Ripple Reduction for DC-DC Converters

Ripple Reduction using Harmonic Notch Filter

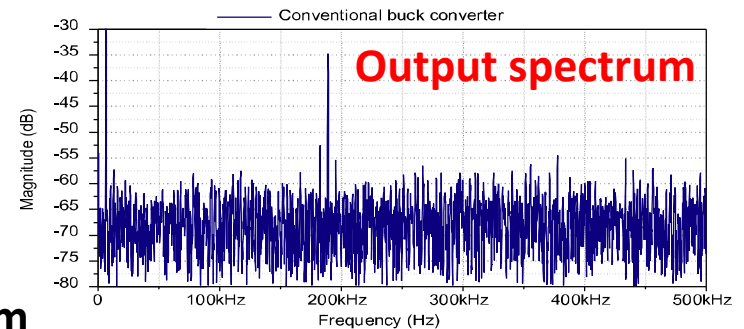
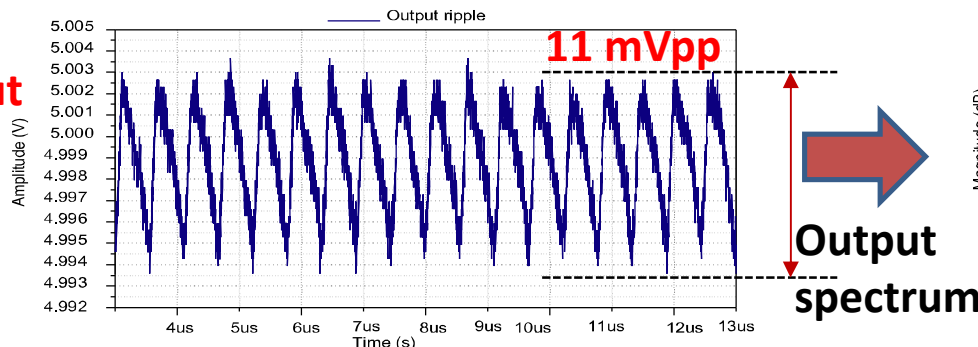
Schematic diagram of DC-DC Buck converter



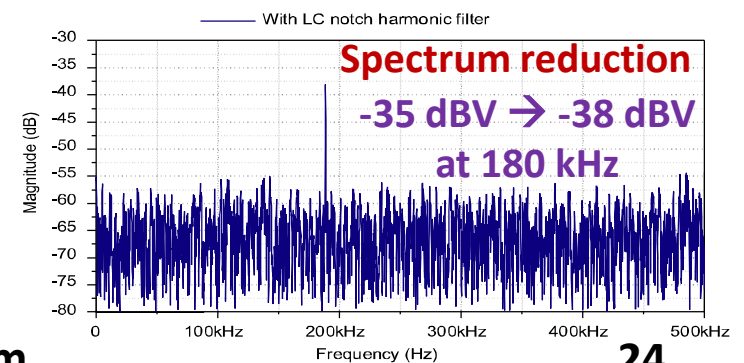
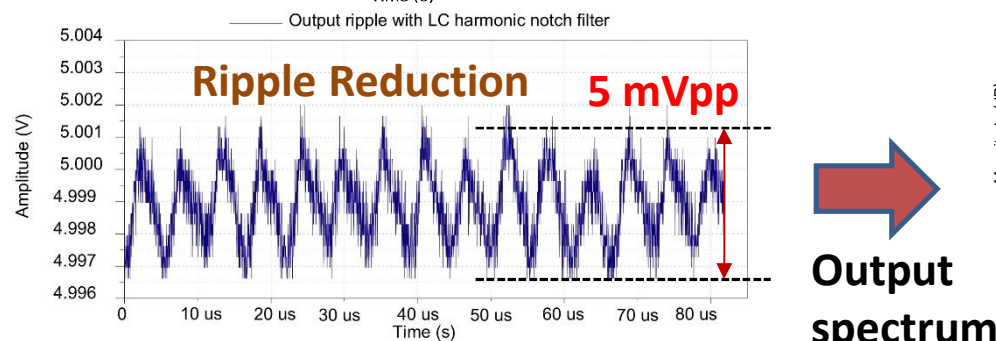
Implemented circuit



Without notch filter



With notch filter



Outline

1. Research Background

- Motivation, objectives and achievements
- Characteristics of an adaptive feedback network

2. Analysis of Power-Stage of DC-DC Converter

- Operating regions of power-stage of DC-DC converter
- Passive parallel RLC network

3. Ripple Reduction for DC-DC Converters

- LC Harmonic Notch filter
- Nichols chart of power stage of buck converter

4. Conclusions

4. Discussion and Comparison

Merits of Self-loop Function Derivation Techniques

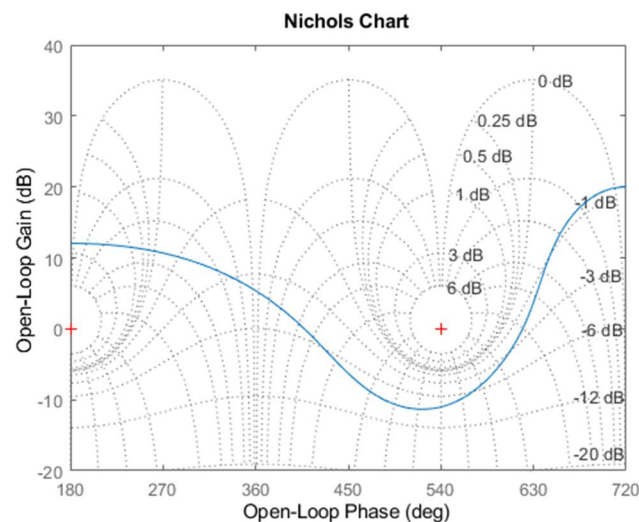
Features	Comparison measurement	Alternating current conservation	Replica measurement	Middlebrook's method
Main objective	Self-loop function	Self-loop function	Loop gain	Loop gain
Transfer function accuracy	Yes	Yes	No	No
Breaking feedback loop	No	Yes	Yes	Yes
Operating region accuracy	Yes	Yes	No	No
Phase margin accuracy	Yes	Yes	No	No
Passive networks	Yes	Yes	No	No

4. Discussion and Comparison

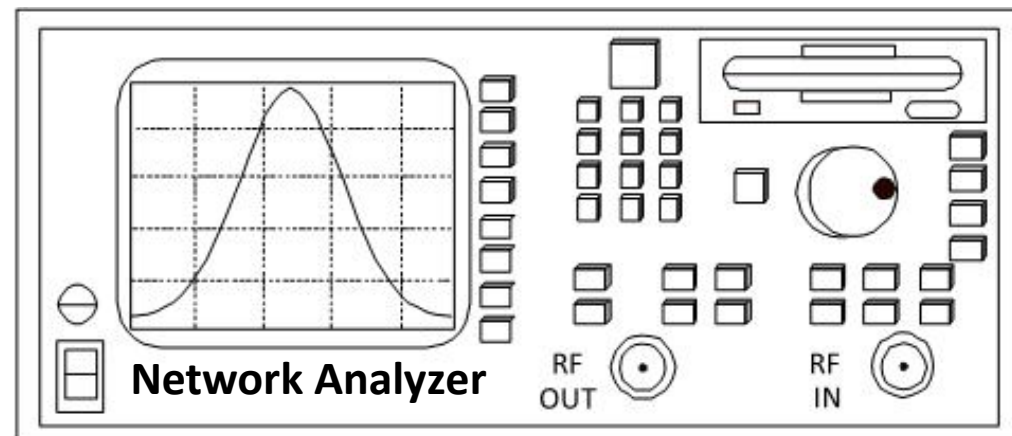
Limitations of Loop Gain on Nichols Charts

- Loop gain is **independent of** frequency variable.
- Loop gain in **adaptive feedback network** is **significantly different from** self-loop function in **linear negative feedback network**.

Nichols chart is **only used** in **MATLAB simulation**.



Nichols chart **isn't** used **widely** in practical measurements (**only used** in control theory).



4. Conclusions

This work:

- Investigation of behaviors of power-stage in DC-DC converters based on alternating current conservation
- Proposed design of passive LC harmonic notch filters for ripple reduction
 - Phase margin improvement from 46 degrees into 49 degrees
 - Ripple reduction from 11 mVpp into 5 mVpp

Future work:

- Stability test for dynamic loads, and parasitic components in printed circuit boards

References

- [1] P. Wang, S. Feng, P. Liu, N. Jiang, X. Zhang, "*Nyquist stability analysis and capacitance selection method of DC current flow controllers for meshed multi-terminal HVDC grids*", J. Power and Energy Systems, pp. 1-13, 2020.
- [2] M. Liu, I. Dassios, G. Tzounas, F. Milano, "*Stability Analysis of Power Systems with Inclusion of Realistic-Modeling of WAMS Delays*", IEEE Trans. Power Systems, Vol. 34(1), pp. 627-636, 2019.
- [3] N. Kumar, V. Mummadi, "*Stability Region Based Robust Controller Design for High-gain Boost DC-DC Converter*", IEEE Trans. Industrial Electronics, Feb. 2020.
- [4] A. Nakhmani, M. Lichtsinder, E. Zeheb, "*Generalized Bode envelopes and generalized Nyquist theorem for analysis of uncertain systems*", Int. J. Robust and Nonlinear Control, Vol. 21(7), pp. 752-767, 2010.
- [5] A. Riccobono, M. Cupelli, A. Monti, E. Santi, T. Roinila, "*Stability of shipboard dc power distribution: Online impedance-based systems methods*", IEEE Electrification Magazine, vol.v5 no. 3, pp. 55-67, Sept. 2017.
- [6] X. Zhang, X. Jiang, Q. Han, "*An improved stability criterion of networked control systems*", Proc. 2010 American Control Conference, Baltimore, USA, July 2010.
- [7] M. Sanz, "*The Nyquist stability criterion in the Nichols chart*", Int. J. Robust and Nonlinear Control, Vol. 26(12), pp. 2643-2651, 2015.
- [8] J. Slater, "*Application of the Nyquist Stability Criterion on the Nichols Chart*", J. Guidance, Control, and Dynamics, Vol. 22 (2), pp. 360-362, 1999.
- [9] X. Jiang, Q. Han, S. Liu, A. Xue, "*A new H stabilization criterion for networked control systems*", IEEE Trans. Autom. Control, Vol. 53(4), pp. 1025–1032, 2008.
- [10] M. Tran, Y. Sun, N. Oiwa, Y. Kobori, A. Kuwana, H. Kobayashi, "*Mathematical Analysis and Design of Parallel RLC Network in Step-down Switching Power Conversion System*", Proc. Int. Conf. Technology and Social Science, Kiryu, Japan, May 2019.
- [11] J. Anagnost, C. A. Desoer, R. Minnichelli, "*Generalized Nyquist Tests for Robust Stability: Frequency Domain Generalizations of Kharitonov's Theorem*", J. Robustness in Identification and Control, pp. 79-96, NY, 1989.
- [12] Y. He, G. Liu, D. Rees, M. Wu, "*Improved stabilization method for networked control systems*", IET Control Theory Applications, Vol. 1(6), pp.1580–1585, 2007.

References

- [13] N. Cohen, Y. Chait, O. Yaniv, C. Borghesa, "*Stability Analysis Using Nichols Charts*", Proc. the 31st IEEE Conf. Decision and Control, Tucson, USA, Dec. 1992.
- [14] A. Riccobono, E. Santi, "*Comprehensive review of stability criteria for dc power distribution systems*", IEEE Trans. Industry Applications, Vol. 50(5), pp. 3525-3535, Sept. 2014.
- [15] C. Peng, M. Fei, "*A refined delay-partitioning approach to the stability of linear systems with interval time-varying delays*", Proc. Int. Symp. Industrial Electronics, Taipei, Taiwan, July 2013.
- [16] K. Liu, E. Fridman, "*Networked-based stabilization via discontinuous Lyapunov functionals*", Int. J. Robust Nonlinear Control, Vol. 22(4), pp. 420–436, 2012.
- [17] R. Middlebrook, "*Measurement of Loop Gain in Feedback Systems*", Int. J. Electronics, vol. 38(4), pp.485-512, 1975.
- [18] M. Tran, A. Kuwana, H. Kobayashi, "*Design of Active Inductor and Stability Test for Ladder RLC Low Pass Filter Based on Widened Superposition and Voltage Injection*", The 8th IIAE Int. Conf. Industrial Application Engineering, Shimane, Japan, March 2020.
- [19] H. Shao, "*Further improvement on delay-dependent stability results for linear systems with time-varying delays*", Proc. 30th Chinese Control Conference, Yantai, China, July 2011.
- [20] X. Zhu, G. Yang, "*New results on stability analysis of networked control systems*", Proc. 2008 American Control Conference, pp.3792–3797, 2008.
- [21] L. Fan, Z. Miao, "*Admittance-Based Stability Analysis: Bode Plots, Nyquist Diagrams or Eigenvalue Analysis*", IEEE Trans. Power Systems, Vol. 35(4), July 2020.
- [22] M. Tran, A. Kuwana, H. Kobayashi, "*Design of Active Inductor and Stability Test for Passive RLC Low Pass Filter*", 10th Int. Conf. Signal and Image Processing, London, UK, July 2020.
- [23] H. Shao, X. Shi, H. Wang, "*Improvements on delay-dependent stability criteria for linear delayed systems*", Proc. 7th Word Conf. Intelligent Control and Automation, Chongqing, China, 2008.
- [24] N. Cohen, Y. Chait, O. Yaniv, C. Borghesani, "*Stability analysis using Nichols charts*" J. Robust and Nonlinear Control, Vol. 39, 1994.
- [25] G. Walsh, H. Ye, L. Bushnell, "*Stability analysis of networked control systems*", IEEE Trans. Control Systems Technology, Vol. 10(3), pp. 438-446, 2002.

*Proceedings of International Conference on
Technology and Social Science 2020
(ICTSS 2020)*

Thank you very much!

ご清聴ありがとうございました。

